Since January 2020 Elsevier has created a COVID-19 resource centre with free information in English and Mandarin on the novel coronavirus COVID-19. The COVID-19 resource centre is hosted on Elsevier Connect, the company's public news and information website.

Journal of Hazardous Materials 396 (2020) 122640

Contents lists available at ScienceDirect

Journal of Hazardous Materials

journal homepage: www.elsevier.com/locate/jhazmat

Determination of Air Filter Anti-Viral Efficiency against an Airborne Infectious Virus

Dae Hoon Park[a], Yun Haeng Joe[b], Amin Piri[a], Sanggwon An[a], Jungho Hwang[a,*]

[a] School of Mechanical Engineering, Yonsei University, Seoul 03722, Republic of Korea
[b] Climate Change Research Division, Korea Institute of Energy Research, Daejeon 34129, Republic of Korea

GRAPHICAL ABSTRACT

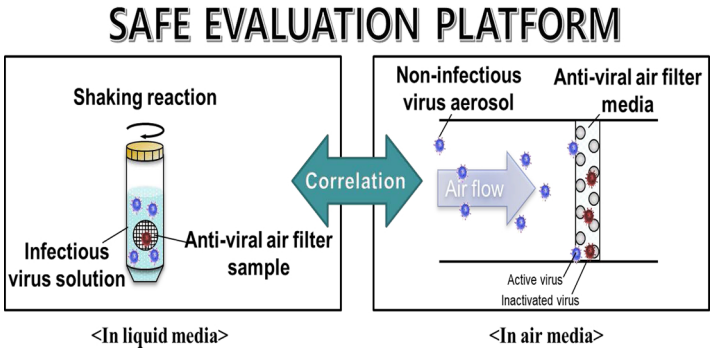

ARTICLE INFO

Editor: R Teresa

Keywords:
Anti-Viral Air Filter
Liquid Media Method
Air Media Method
Bioaerosols
Safe Evaluation Platform

ABSTRACT

Recently, various studies have reported the prevention and treatment of respiratory infection outbreaks caused by lethal viruses. Consequently, a variety of air filters coated with antimicrobial agents have been developed to capture and inactivate virus particles in continuous airflow conditions. However, since aerosolized infectious viral-testing is inadvisable due to safety concerns, their anti-viral capability has only been tested by inserting the filters into liquid media, where infectious virus particles disperse. In this study a novel method of determining anti-viral performance of an air filter against airborne infectious viruses is presented. Initially, anti-viral air filter tests were conducted. Firstly, by an air-media test, in which the air filter was placed against an aerosolized non-infectious virus. Secondly, by a liquid-media test, in which the filter was inserted into a liquid medium containing a non-infectious virus. Subsequently, a correlation was established by comparing the susceptibility constants obtained between the two medium tests and an association was found for the air medium test with infectious virus. After ensuring the relationship did not depend on the virus species, the correlation was used to derive the results of the air-medium test from the results of the liquid-medium test.

1. INTRODUCTION

Biologically originated aerosols generally involve fungi, bacteria, and viruses and are defined as bioaerosols. In human environments, bioaerosol contaminants can cause adverse health impacts, such as allergic, infectious, and toxigenic diseases [1–4]. Recently, many researchers have published works on the prevention and treatment of respiratory infection outbreaks caused by lethal viruses, such as the

* Corresponding author.
E-mail address: hwangjh@yonsei.ac.kr (J. Hwang).

https://doi.org/10.1016/j.jhazmat.2020.122640
Received 15 January 2020; Received in revised form 17 March 2020; Accepted 2 April 2020
Available online 12 April 2020

Middle East respiratory syndrome [5,6], severe acute respiratory syndrome coronavirus [7,8], novel swine-origin influenza A (H1N1; cause of swine flu) [9,10], and, very recently, novel coronavirus (2019-nCoV) first detected in Wuhan, China [11,12]. A variety of air filters coated with antimicrobial agents have been developed to capture and inactivate virus particles under continuous airflow conditions [13–19].

Lee et al. [20] assessed the anti-viral performance of an iodine (I_2)-releasing filter medium as a protective device against airborne pathogens by using MS2 aerosols. Rengasamy et al. [21] evaluated the efficacies of surgical filters treated with four different antimicrobial agents (silver-copper, EnvizO_3-Shield, iodine-activated resin, and TiO_2) against aerosolized MS2 virus-containing droplet nuclei. Woo et al. [22] investigated the inactivated performance of dialdehyde cellulose filters against an airborne MS2 virus with various treatment times. Our group has investigated air filter coatings using different nanoparticles (NPs) and studied their anti-viral efficiencies against viruses captured by the filter. In our previous works, tests were conducted with non-infectious viruses for safety reasons. Joe et al. [23] fabricated an anti-viral filter using an aerosol coating of silica hybrid particles decorated with silver NPs (SiO_2-Ag) and conducted an anti-viral ability test against the aerosolized bacteriophage MS2 virus. Furthermore, Park et al. [24] developed an instrument for dry coating a commercial air filter unit with a large number of SiO_2-Ag NPs. They evaluated the filtration capability and anti-viral activity of the instrument against the aerosolized bacteriophage MS2. Moreover, Park et al. [25] coated a glass fiber filter medium with carbon nanotubes (CNTs) and performed an inactivation test against the bacteriophage MS2 virus. Joe et al. [26] evaluated the anti-viral efficiency of a silver (Ag) NP coated air filter against the bacteriophage MS2 virus through the process of dust loading. In all the abovementioned works, the bacteriophage MS2 virus was aerosolized using an atomizer or nebulizer, delivered to a filter by forced convection flow, and collected on the filter surface. The collected virus particles were then eluted from the filter surface to a liquid medium containing *Escherichia coli* strain C3000 (as the host of the bacteriophage MS2 virus) through physical vibration (sonication, vortex, and shaking) or elution with a urea-arginine phosphate buffer (U-APB) solution. Subsequently, plaque counting was performed, thereby enabling the evaluation of the effect of the NPs coated on the filter on the viability of the virus particle.

Nonetheless, the test mentioned above (hereafter termed the air media test) may not be recommended for airborne infectious viruses due to the possibility of aerosol transmission [27–29]. In addition, because airborne virus particles move with airflow and can be captured by air filters used in indoor air cleaning, the data from the air media test are more practical and useful to people who need to use the air filters, such as healthcare workers [30,31]. This paper presents a novel method of determining the anti-viral capability of an air filter against an airborne infectious virus. First, an Ag NP coated filter was inserted into a liquid medium in which infectious virus particles (H1N1) were dispersed. Then, the plaque counting method was conducted, hereafter termed the liquid media test. The results of the liquid media test were then converted to those of the air media test by using a correlation equation, which was established by comparing the susceptibility constants obtained from the two media tests with the selected non-infectious virus particles. Susceptibility has been used to explain the relative importance of various parameters affecting antimicrobial efficiency, such as the coating areal density of Ag NPs on the filter surface. Yoon et al. [32] used the susceptibility constant to evaluate the antibacterial effects of Ag and Cu NPs.

2. MATERIALS AND METHODS

2.1. Preparation of air filter coated with Ag NPs

The anti-viral air filters in this study were prepared by coating glass fiber high-efficiency particulate air (HEPA) filters (Fabriano, Italy) with Ag NPs. The HEPA filters of thickness 0.07 ± 0.004 cm, solidity 0.09 ± 0.004, and fiber diameter 2.7 ± 0.55 μm were used. Ag NPs were synthesized using a lab-made spark discharge generation system. The details of the coating process have been presented in Joe et al. [26]. The size distribution of NPs was measured by scanning mobility particle sizer (SMPS), and the range of the NP coating areal densities used was 1.1×10^{10}–1.4×10^{11} particles cm^{-2} of the filter. To confirm the evolution and composition of the Ag NPs on the filter fibers, field emission scanning electron microscope-energy dispersive X-ray (FESEM-EDX; JSM-7610F-Plus, JEOL, Japan) analyses were performed.

2.2. Preparation of test virus solutions

In this study, *Escherichia coli* bacteriophage T1 (ATCC 11303-B1), T4 bacteriophage (ATCC 11303-B4), and MS2 bacteriophage (ATCC 15597-B1) were used as the non-infectious virus species. These viruses were selected because they are relatively safe to handle in a biosafety level (BSL) I laboratory. These bacteriophages have been used in previous research works as surrogates for human and animal respiratory viruses [33–35] and in stringent test cases to evaluate the efficacy of antimicrobial agents [36,37]. Each virus solution was prepared using 0.1 mL of virus stock defrosted at room temperature and poured into 50 mL of deionized (DI) water. To measure the bacteriophage concentration of the stock, a plaque assay was used (initial concentration: 10^{11} plaque forming unit per milliliter [PFU mL^{-1}]). The infectious virus species H1N1 (influenza A/California/07/2009) was used as provided by BioNano Health-Guard Research Center, Daejeon, Korea (initial concentration: 2.76×10^7 PFU mL^{-1}) [38]. Moreover, experiments involving H1N1 viruses were performed inside a Class II (laminar flow) Biosafety Cabinet (Type A1, KUMKANGENG Inc., Korea) in a BSL II laboratory.

2.3. Air media test with non-infectious virus

As shown in Fig. 1, the aerosolized virus particles were deposited onto an air filter sample (1 cm in diameter) during the time of deposition, (τ), (Step 1). Then, the prepared non-infectious virus solution was aerosolized using an atomizer (9302, TSI Inc., USA) with a 2 L min^{-1} flow rate of compressed clean air, after which the aerosolized virus particles entered a test duct in which a prepared anti-viral air filter (see Section 2.1) was installed with a diffusion dryer for moisture removal. The pressure and temperature were maintained at standard atmospheric conditions, whereas the relative humidity was maintained at approximately 38%. The two aerosol sampling probes were placed before and after the filter in the test duct. The aerosolized virus concentrations upstream (N_{up}) and downstream (N_{down}) of the filter were measured by an SMPS, which consisted of a classifier controller (3080, TSI Inc., USA), a differential mobility analyzer (DMA, 3085, TSI Inc., USA), an ultrafine condensation particle counter (UCPC, 3776, TSI Inc., USA), and an aerosol charge neutralizer (Soft X-ray charger 4530, HCT Co., Ltd., Korea). The SMPS measured the electrical mobility diameter of aerosol particles between 4 and 165 nm and operated with a sample flow rate of 0.3 L min^{-1} and a scan time of 120 s.

The concentration of virus particles on the filter sample (C_{air}) was calculated using the following equation:

$$C_{air} = \frac{(N_{up} - N_{down}) \times Q \times \tau}{A_{filter}} \, [particles\ cm^{-2}] \quad (1)$$

where Q represents the airflow rate (L min^{-1}) and A_{filter} represents the filter sample surface area (cm^2). The number of virus particles deposited onto the filter per unit volume of air passing through the filter was calculated as ($N_{up} - N_{down}$). The selected deposition time (τ) was 10 min.

After the aerosolized virus particles were deposited onto the air filter sample, the filter sample was placed in an incubator. The air

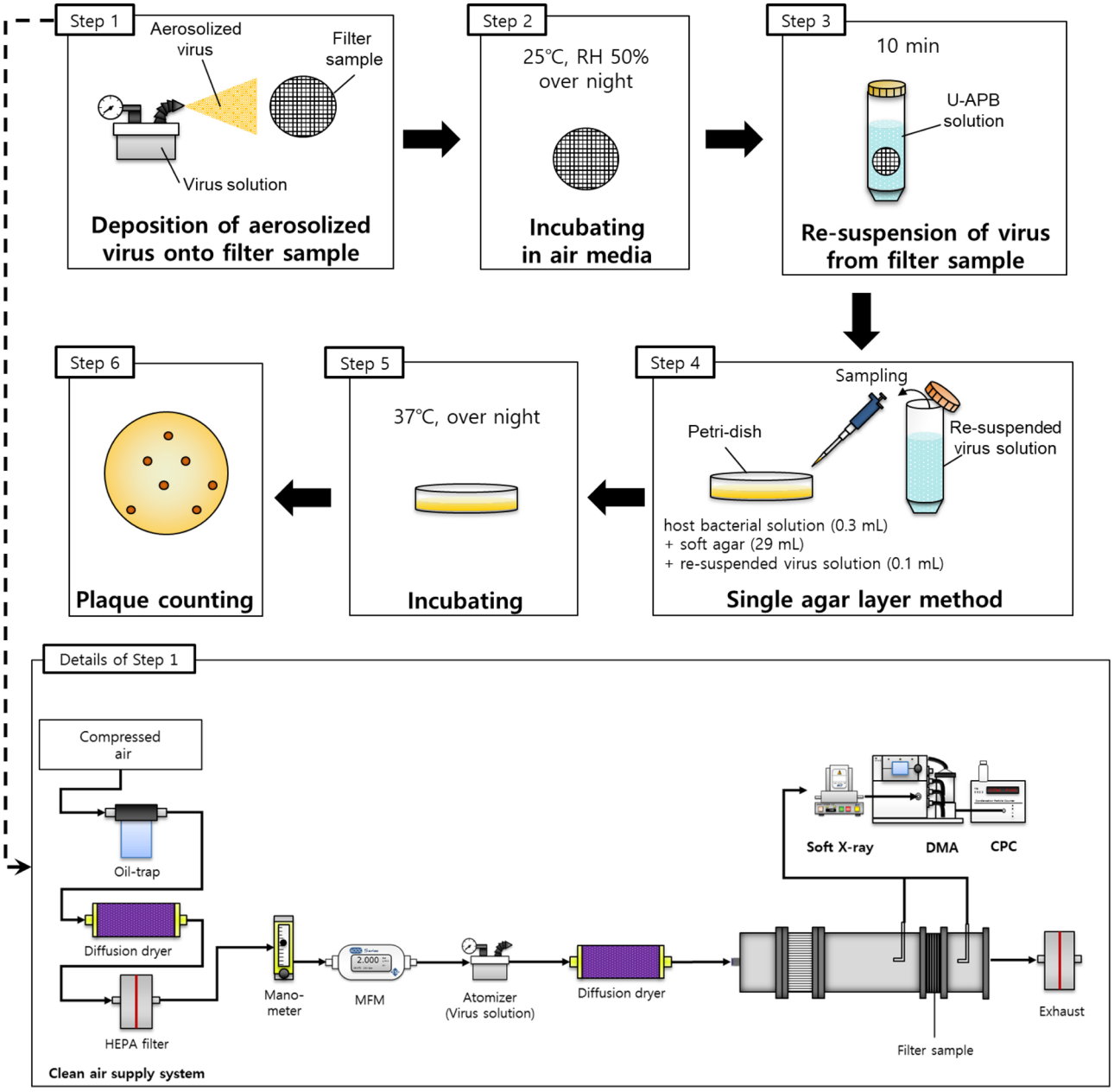

Fig. 1. Experimental steps for assessing anti-viral capability in air media.

temperature and relative humidity inside the incubator were maintained at 25 °C and 50%, respectively (Step 2). Following overnight incubation, each filter was submerged in 1 mL of RNase-free U-APB solution, which was prepared by adding 0.9 g of urea, 0.4 mL of 0.2 M NaH_2PO_4, and 0.5 M L-arginine into a 10-mL solution of DI water for 10 min to detach the deposited virus particles from the filter sample [39] (Step 3). Subsequently, the single-layer method was used to record the number of virus particles in the U-APB solution [40] by mixing the 0.1 mL of the solution with the 0.3 mL of host bacterial solution and 29 mL of soft agar that was maintained at 48 °C. Accordingly, the mixture was poured into a petri-dish (Step 4), and, following overnight incubation at 37 °C (Step 5), the number of plaques was recorded (Step 6). Finally, the overall anti-viral efficiency of the filter sample was calculated according to the following equation:

$$\bar{\eta}_{antiviral} = 1 - \frac{PFU}{PFU_0}, \tag{2}$$

where PFU indicates the concentration of virus particles and the subscript 0 indicates the pristine filter. The test results were then compared with the theoretical predictions about the overall anti-viral efficiency, as determined per the following equation:

$$\bar{\eta}_{antiviral} = 1 - \phi_{surv,\tau}. \tag{3}$$

The fraction of surviving virus particles ($\phi_{surv,\tau}$) during the time interval τ was defined by Joe et al. [26].

$$\phi_{surv,\tau} = \exp\left[-\kappa\frac{\rho_{agent}}{\Gamma_{depo}\tau}\right] + \frac{\kappa\rho_{agent}}{\Gamma_{depo}\tau}Ei\left[-\kappa\frac{\rho_{agent}}{\Gamma_{depo}\tau}\right], \tag{4}$$

where ρ_{agent} represents the areal density of the Ag NP coating on the filter surface (particles cm^{-2}) and τ indicates the time during which the virus particles were deposited onto the filter (10 min in this study). The variable κ is a dimensionless fitting parameter. Moreover, Joe et al. [26] reported that κ represents the susceptibility of a virus species against an anti-viral agent and, therefore, depends on the type of virus and anti-viral agent. The variable Γ_{depo} represents the virus deposition

flux onto the filter (particles $cm^{-2} min^{-1}$), which was equal to $(N_{up} - N_{down})Q/A_{filter}$. The function $Ei(z)$ represents the exponential integral function and is defined as:

$$Ei(z) = -\int_{-z}^{\infty} \frac{e^{-t}}{t} dt. \quad (5)$$

The filter sample detachment efficiency ($\eta_{detachment}$) for the deposited virus particles was approximately 30% (Fig. S1). Additional anti-viral effects from the released materials (such as Ag NPs and/or Ag ions) during the elution process were negligible (Fig. S2). The experimental steps (Fig. 1) were repeated with varying areal densities of Ag NP coating onto the filter sample.

2.4. Liquid media test with non-infectious virus

Regarding the liquid media test, an air filter sample, which contained non-infectious virus particles, was obtained using the procedure presented in Section 2.3. Therefore, the total number of virus particles deposited onto the filter sample during the deposition time (τ) could be expressed as $(N_{up} - N_{down})Q\tau$. The filter sample was submerged in an RNase-free U-APB solution for 10 min to detach the deposited virus particles from the filter sample. Next, the single agar layer method was used to count the number of virus particles in the U-APB solution. After overnight incubation at 37 °C, the number of plaques was counted. The ratio between the number of virus particles detached from the filter sample, $(N_{up} - N_{down})Q\tau\eta_{detachment}$, and the number of plaques, P_{virus}, is expressed as:

$$\frac{(N_{up} - N_{down}) \times Q \times \tau \times \eta_{detachment}}{P_{virus}} = \gamma \ [particles\ PFU^{-1}] \quad (6)$$

where γ represents a constant dependent on the virus particle species.

The concentration of virus particles on the filter sample in the liquid media (C_{liquid}) was calculated according to the following equation:

$$C_{liquid} = \frac{C_{virus\ solution} \times V_{virus\ solution}}{A_{filter}} \ [PFU\ cm^{-2}] \quad (7)$$

where $C_{virus\ solution}$ indicates the virus concentration of the virus solution (PFU mL^{-1}) and $V_{virus\ solution}$ represents the volume of the virus solution (mL). Therefore, Equation (7) can be rewritten as:

$$C_{liquid} = \frac{C_{virus\ solution} \times V_{virus\ solution}}{A_{filter}} \times \gamma \ [particles\ cm^{-2}] \quad (8)$$

The value of C_{liquid} was adjusted to equal that of C_{air} by controlling for $C_{virus\ solution}$.

The experimental steps used to evaluate the anti-viral capability of the filter in the liquid media are illustrated in Fig. 2. This test used a virus solution that was diluted with DI water (10^8 PFU mL^{-1} for MS2, T1, and T4 bacteriophages). First, a circular filter sample of 1 cm in diameter was placed into the solution (Step 1). Then, the solution was incubated and shook at 37 °C for 24 h (Step 2). Afterward, the solution was continually diluted with DI water to acquire a countable number of plaques, and the number of virus particles was then evaluated using the single agar layer method (Step 3). After overnight incubation at 37 °C (Step 4), the number of plaques was counted (Step 5). Finally, the overall anti-viral efficiency was calculated using Equation (2). The experimental steps shown in Fig. 2 were repeated with various areal densities of the Ag NP coating on the filter sample.

2.5. Liquid media test with infectious virus (H1N1)

Fig. 3 illustrates the experimental steps undertaken to evaluate the anti-viral capacity of the filter. The liquid media test was conducted with H1N1, using a virus solution that was diluted with DI water to a concentration of 10^6 PFU mL^{-1}. Similar to a previously reported procedure, a filter sample was cut into a 1-cm diameter circular shape and placed into the solution (Step 1). Then, the solution was incubated and shook at 37 °C for 24 h (Step 2). Next, the live H1N1 viruses were quantified using an RNA amplifying method. The reverse transcription-polymerase chain reaction (RT-PCR) system (12675885, Thermo Scientific™ PikoReal™, UK) was used to amplify the RNA of the virus (Step 3). Finally, the overall anti-viral efficiency was determined according to the cycle number obtained from the PCR analysis, as follows:

$$\bar{\eta}_{antiviral} = 1 - \frac{1}{2^{C_i - C_0}}, \quad (9)$$

where C_i indicates the cycle number for the Ag NP coated filter and C_0 represents the cycle number for the pristine filter (Step 4). The experiments were repeated with various areal densities of the Ag NP coating.

2.6. Air media test with infectious virus (H1N1)

To demonstrate the validity of the correlation for infectious viruses, additional air media tests with infectious virus H1N1 were carefully performed in a BSL II laboratory while upholding BSL III precautions (Fig. S4).

3. RESULTS AND DISCUSSION

3.1. Preparation of air filter coated with Ag NP

Fig. 4 demonstrates the size distributions of aerosolized Ag NPs measured upstream and downstream of the filter with the SMPS. The geometric mean diameter (GMD) and geometric standard deviation (GSD) of the NPs were approximately 17.5 nm and 1.69, respectively. Because of the high filtration efficiency of the HEPA filter, the coating efficiency was more than 99.99%. Fig. 4 also contains scanning electron microscopy (SEM) images of the coated filter with increasing coating areal density. This figure illustrates that the Ag NPs were well distributed on the glass fibers and the amounts of Ag NPs were well matched with the coating areal densities. Moreover, the SEM images clearly show that the depth deposition was the dominant filtration mechanism for the filter media because of the use of the micrometer fibers [41]. The high oxidation rate of NPs on the glass fibers was observed in EDX data (in Fig. 4), indicating that the ambient clean air used in the coating process would oxidize the resulting particles.

3.2. Air and liquid media tests with non-infectious virus

The size distributions of non-infectious viruses are shown in Fig. S5a, b, and c. The GMDs of the aerosolized virus particles for MS2, T1, and T4 were 19.8, 23.1, and 24.6 nm, respectively. The GSDs were 1.74–1.93. In each case, the filtration efficiency of the air filter was more than 99.99%. Fig. 5 shows the air media test results for $\bar{\eta}_{antiviral}$ (see Equation (2)) with various Ag NP coating areal densities, in which the MS2 bacteriophage was used. In addition, Fig. 5 shows the liquid media test results for $\bar{\eta}_{antiviral}$ with various NP coating areal densities. Because $\Gamma_{depo}\tau = C_{air} = C_{liquid}$, Equation (3) was also applied to the liquid media test. The value of $\bar{\eta}_{antiviral}$ for each media test increased and became saturated as the areal density of the coating increased. Notably, the $\bar{\eta}_{antiviral}$ for the liquid media test was lower than the $\bar{\eta}_{antiviral}$ for the air media test, implying that $\kappa_{liq} < \kappa_{air}$. In other words, the virus particles are more susceptible to Ag NPs in air media than in liquid media. One plausible reason for this could be that in the air media test, many of the virus particles may have directly contacted the Ag NPs after being deposited and fixed onto the surface of the filter. On the contrary, in the liquid media test, virus particles could move freely in the liquid, enabling many virus particles to avoid contact with the Ag NPs. Specifically, the chances for virus particles to interact with Ag NPs were higher in the air media than in the liquid media tests.

In the work of Yoon et al. [32], the susceptibility constant (Z) for estimating antimicrobial activities of the NPs was suggested as follows:

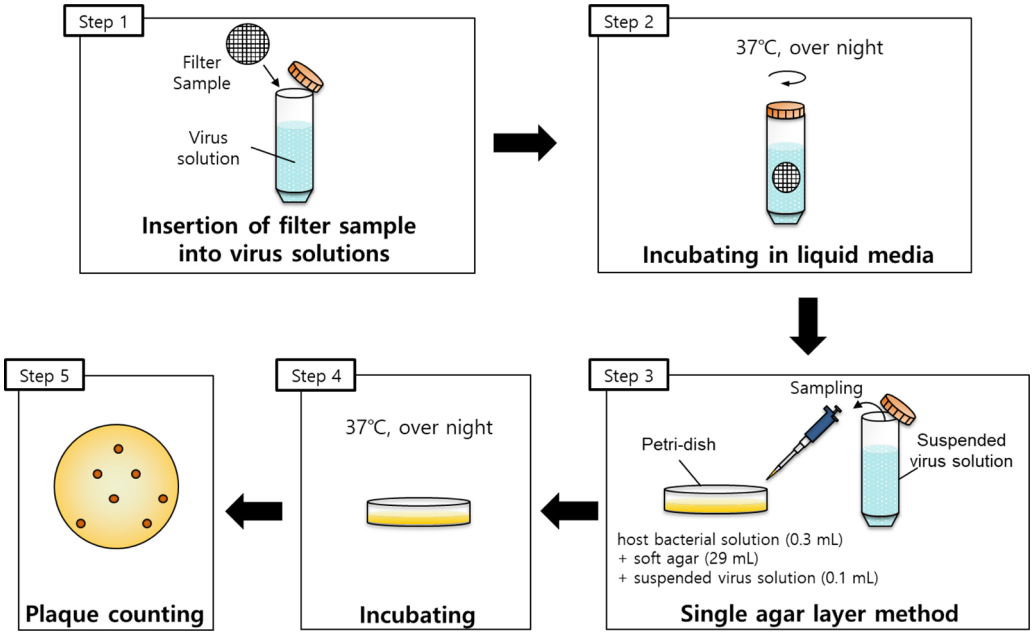

Fig. 2. Experimental steps for assessing anti-viral capability in liquid media.

$$Z = \frac{-\ln(N/N_0)}{C}\,[mL\,\mu g^{-1}] \tag{10}$$

where C is the concentration of NPs (μg mL^{-1}) and (N/N_0) is the survival fraction of the microorganism. In this study, the following equation was applied to assess the anti-viral capability of the filter against a non-infectious virus species:

$$Z = \frac{-\ln(PFU\ /PFU_0)}{\rho_{agent}}\,[cm^2\ particles^{-1}]. \tag{11}$$

The experimental results for PFU/PFU_0 (survival fraction), as shown in Fig. 5, are re-plotted in Fig. 6. In Fig. 6, curve fits were attained by substituting the experimentally determined susceptibility constants into Equation (11) and then calculating the corresponding survival fractions. The correspondence between the curve fits and the experimental results are represented by R^2 values of 0.985 and 0.935 for liquid media and air media tests, respectively. The susceptibility constants, Z_{liquid} and Z_{air}, were 3.94×10^{-11} and 2.00×10^{-10} cm^2 $particles^{-1}$, respectively. As anticipated, the susceptibility constant of the air media test was higher than that of the liquid media test. An explicit correlation was found between the two susceptibility constants, expressed as follows:

$$Z_{liquid} = \beta Z_{air}, \tag{12}$$

where β represents a constant dependent on species of virus particles

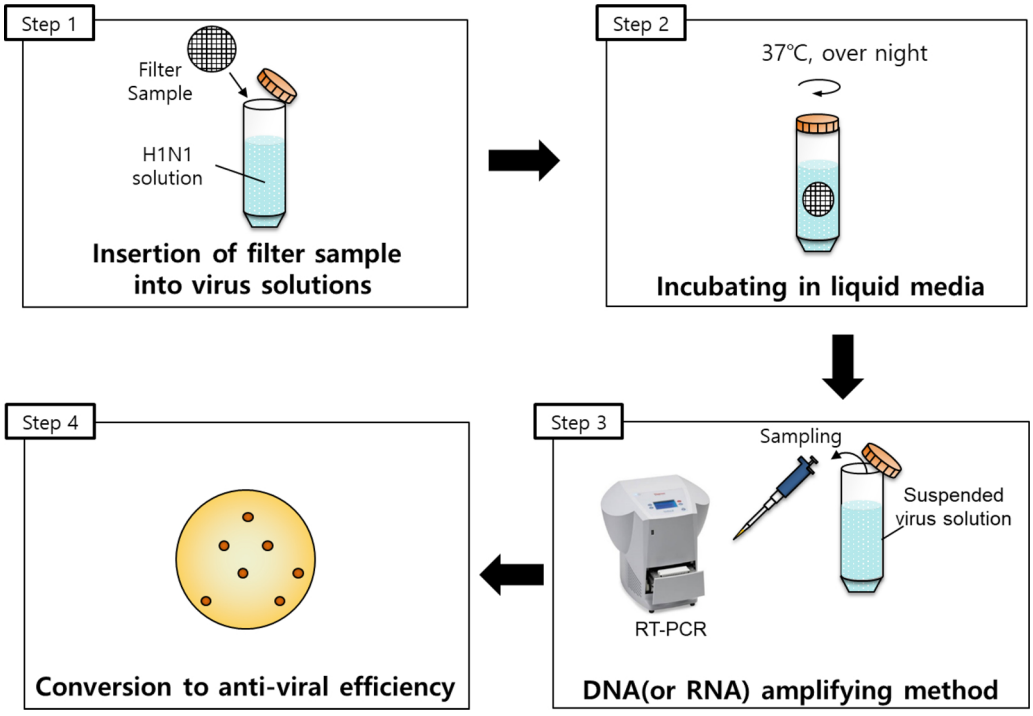

Fig. 3. Experimental steps for assessing anti-viral capability against the H1N1 virus in liquid media.

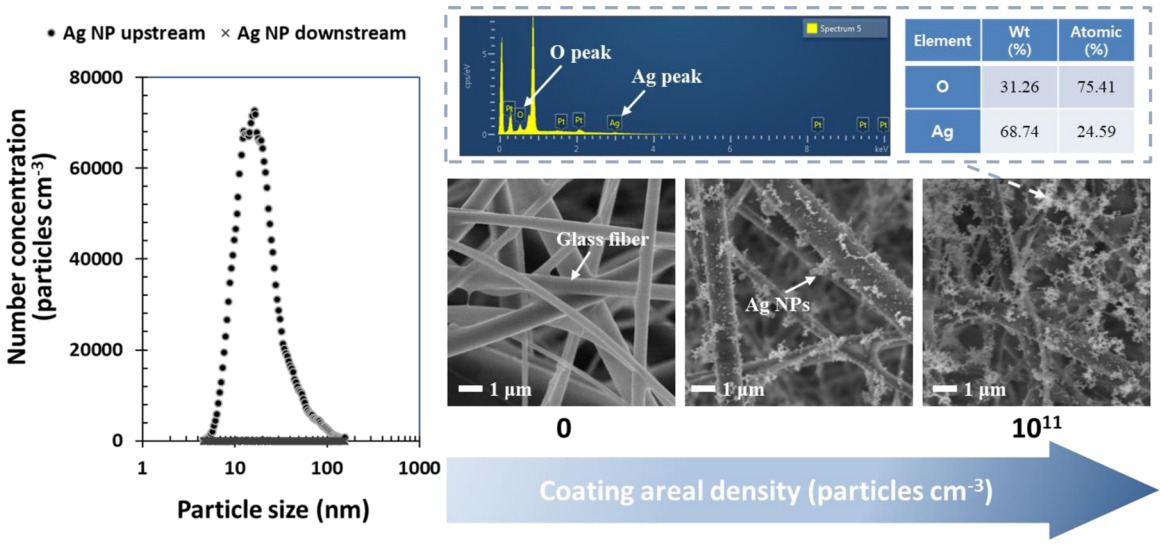

Fig. 4. Size distributions of aerosolized silver nanoparticles (Ag NPs) measured upstream and downstream of the filter by using the scanning mobility particle sizer (SMPS) (left). The scanning electron microscopy-energy dispersive X-ray (SEM-EDX) data of the coated filter with increasing coating areal densities (right).

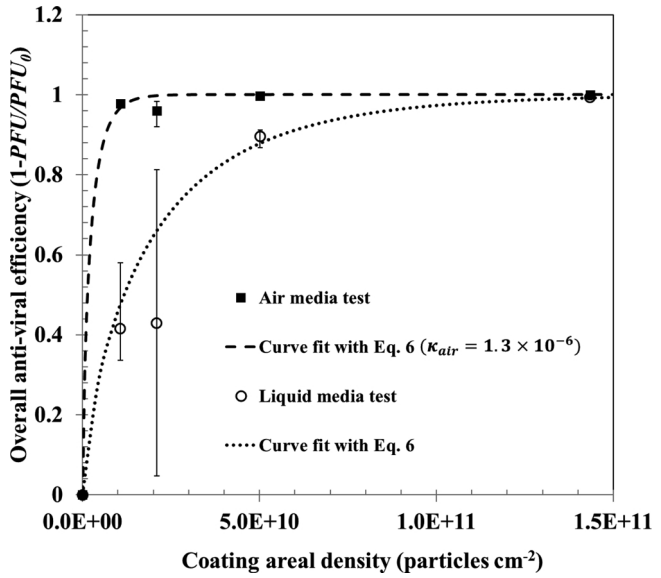

Fig. 5. Overall anti-viral efficiency of the fabricated filter with various coating areal densities in liquid and air media (using the MS2 bacteriophage).

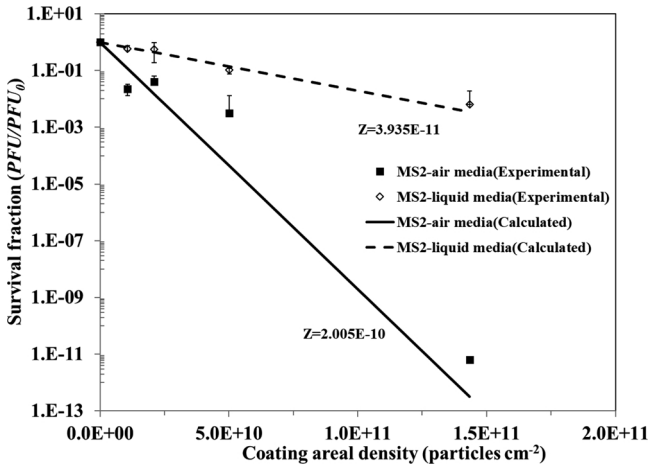

Fig. 6. Survival fractions of MS2 bacteriophage against silver nanoparticles (Ag NPs) with various coating areal densities in both media types. Symbol: experimental data. Line: calculation by Equation (11).

and anti-viral agent NPs. The experimental results for the MS2 bacteriophage were predicted by Equation (12) when β was set to 0.196. The values of β for the *E. coli* bacteriophage T1 and the T4 bacteriophage were found to be 0.2 and 0.198, respectively (Fig. S3). Although the three virus types had different sizes, the values of β were similar at approximately 0.2 (Fig. S3).

3.3. Liquid media test with infectious virus (H1N1)

The liquid media test was performed with the infectious virus H1N1. After converting the results of the liquid media test to those of the air media test by using the correlation equation, we were able to evaluate the effect of the Ag NPs on the infectious virus. The survival fraction of the H1N1 virus is shown in Fig. 7. The susceptibility constant of the liquid media test, Z_{liquid}, was 6.96×10^{-11} cm^2 particles^{-1}, which resulted in an air media test susceptibility constant (Z_{air}) of 3.48×10^{-10} cm^2 particles^{-1}. This implied that its anti-viral effectiveness could be underestimated in the liquid media test in comparison with the air media test.

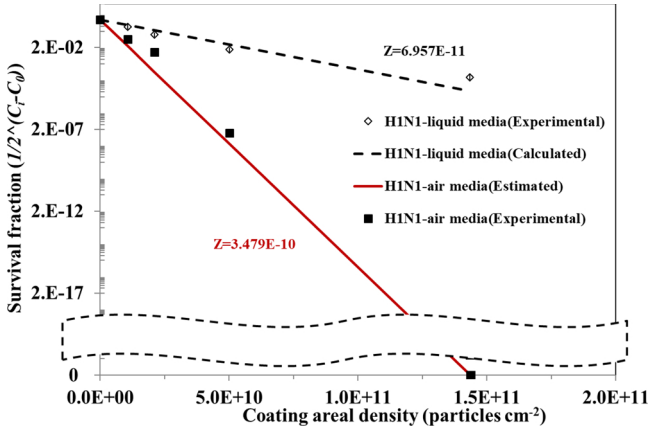

Fig. 7. Survival fractions of infectious virus against silver nanoparticles (Ag NPs) with various coating areal densities. Symbol: experimental data. Line: calculation by Equation (11).

3.4. Air media test with infectious virus (H1N1)

Interestingly, the estimated susceptibility constant and survival fraction from the proposed correlation matched with the experimental data with aerosolized H1N1 particles, which had a GMD of 39.6 nm in diameter and a GSD of 1.76 (Fig. S5d). Thus, it was confirmed that the results obtained from non-infectious virus experiments could be applied to those of the infectious virus (Fig. 7).

This study demonstrated an efficient and reasonable method to determine the anti-viral efficiency of an air filter against an airborne infectious virus without directly testing with an aerosolized infectious virus.

4. CONCLUSIONS

In conclusion, our method determined two major filter operation characteristics: (1) anti-viral capabilities of various anti-viral filters under continuous airflow conditions can be evaluated by performing an anti-viral test in a liquid medium without aerosolizing virus particles and (2) anti-viral capabilities can be quantitatively compared by comparing κ values (where a higher κ value corresponds to a higher anti-viral capability). Through testing conducted in liquid media, these results can be a basis for further fundamental research on predicting the viability of human-infectious viruses that can cause respiratory diseases in air media.

CRediT authorship contribution statement

Dae Hoon Park: Conceptualization, Methodology, Validation, Formal analysis, Investigation, Resources, Writing - original draft, Writing - review & editing. **Yun Haeng Joe:** Validation, Investigation. **Amin Piri:** Investigation, Visualization. **Sanggwon An:** Investigation, Writing - review & editing. **Jungho Hwang:** Writing - review & editing, Supervision, Project administration.

Declaration of Competing Interest

The authors declare that they have no known competing financial interests or personal relationships that could have appeared to influence the work reported in this paper.

Acknowledgments

This research was supported by Basic Science Research Program through the National Research Foundation of Korea (NRF) funded by the Ministry of Science, ICT and future Planning (NRF-2018R1A2A1A05020683).

Appendix A. Supplementary data

Supplementary material related to this article can be found, in the online version, at doi:https://doi.org/10.1016/j.jhazmat.2020.122640.

References

Douwes, J., Thorne, P., Pearce, N., Heederik, D., 2003. Bioaerosol health effects and exposure assessment: progress and prospects. Annals of Occupational Hygiene 47 (3), 187–200.

Grinshpun, S.A., Adhikari, A., Honda, T., Kim, K.Y., Toivola, M., Ramchander Rao, K.S., Reponen, T., 2007. Control of aerosol contaminants in indoor air: combining the particle concentration reduction with microbial inactivation. Environmental Science & Technology 41 (2), 606–612.

Hong, T., Gurian, P.L., 2012. Characterizing bioaerosol risk from environmental sampling. Environmental Science & Technology 46 (12), 6714–6722.

Yao, M., 2018. Bioaerosol: A bridge and opportunity for many scientific research fields. Journal of Aerosol Science 115, 108–112.

Cho, S.Y., Kang, J.M., Ha, Y.E., Park, G.E., Lee, J.Y., Ko, J.H., Lee, Y.J., Kim, J.M., Kang, C.-I., Jo, I.J., Ryu, J.G., Choi, J.R., Kim, S., Huh, H.J., Ki, C.-S., Kang, E.-S., Peck, K.R., Dhong, H.-J., Song, J.-H., Chung, D.R., Kim, Y.-J., 2016. MERS-CoV outbreak following a single patient exposure in an emergency room in South Korea: an epidemiological outbreak study. The Lancet 388 (10048), 994–1001.

Adhikari, U., Chabrelie, A., Weir, M., Boehnke, K., McKenzie, E., Ikner, L., Wang, M., Wang, Q., Young, K., Haas, C.N., Rose, J., Mitchell, J., 2019. A Case Study Evaluating the risk of infection from Middle Eastern Respiratory Syndrome Coronavirus (MERS-CoV) in a Hospital Setting Through Bioaerosols. Risk Analysis 39 (12), 2608–2624.

Booth, T.F., Kournikakis, B., Bastien, N., Ho, J., Kobasa, D., Stadnyk, L., Mederski, B., 2005. Detection of airborne severe acute respiratory syndrome (SARS) coronavirus and environmental contamination in SARS outbreak units. Journal of Infectious Diseases 191 (9), 1472–1477.

Yu, I.T., Li, Y., Wong, T.W., Tam, W., Chan, A.T., Lee, J.H., Ho, T., 2004. Evidence of airborne transmission of the severe acute respiratory syndrome virus. New England Journal of Medicine 350 (17), 1731–1739.

Fabian, P., McDevitt, J.J., DeHaan, W.H., Fung, R.O., Cowling, B.J., Chan, K.H., Milton, D.K., 2008. Influenza virus in human exhaled breath: an observational study. PloS One 3 (7), e2691.

Smith, G.J., Vijaykrishna, D., Bahl, J., Lycett, S.J., Worobey, M., Pybus, O.G., Ma, S.K., Cheung, C.L., Raghwani, J., Bhatt, S., 2009. Origins and evolutionary enomics of the 2009 swine-origin H1N1 influenza A epidemic. Nature 459, 1122–1125.

Wu, F., Zhao, S., Yu, B., Chen, Y.M., Wang, W., Song, Z.G., Hu, Y., Tao, Z.W., Tian, J.H., Pei, Y.Y., Yuan, M.L., Zhang, Y.L., Dao, F.H., Liu, Y., Wang, Q.M., Zheng, J.J., Xu, L., Holmes, E.C., Zhang, Y.Z., 2020. A new coronavirus associated with human respiratory disease in China. Nature 579, 265–269.

Huang, C., Wang, Y., Li, X., Ren, L., Zhao, J., Hu, Y., Zhang, L., Fan, G., Xu, J., Gu, X., Cheng, Z., Yu, T., Xia, J., Wei, Y., Wu, W., Xie, X., Yin, W., Li, H., Liu, M., Xiao, Y., Gao, H., Guo, L., Xie, J., Wang, G., Jiang, R., Gao, Z., Jin, Q., Wang, J., Cao, B., 2020. Clinical features of patients infected with 2019 novel coronavirus in Wuhan, China. The Lancet. 395 (10223), 497–506.

Jung, J.H., Hwang, G.B., Lee, J.E., Bae, G.N., 2011. Preparation of airborne Ag/CNT hybrid nanoparticles using an aerosol process and their application to antimicrobial air filtration. Langmuir 27 (16), 10256–10264.

Rahaman, M.S., Vecitis, C.D., Elimelech, M., 2012. Electrochemical carbon-nanotube filter performance toward virus removal and inactivation in the presence of natural organic matter. Environmental Science & Technology 46 (3), 1556–1564.

Demir, B., Cerkez, I., Worley, S.D., Broughton, R.M., Huang, T.S., 2015. N-halamine-modified antimicrobial polypropylene nonwoven fabrics for use against airborne bacteria. ACS Applied Materials & Interfaces 7 (3), 1752–1757.

Choi, J., Yang, B.J., Bae, G.N., Jung, J.H., 2015. Herbal extract incorporated nanofiber fabricated by an electrospinning technique and its application to antimicrobial air filtration. ACS Applied Materials & Interfaces 7 (45), 25313–25320.

Sim, K.M., Park, H.S., Bae, G.N., Jung, J.H., 2015. Antimicrobial nanoparticle-coated electrostatic air filter with high filtration efficiency and low pressure drop. Science of The Total Environment 533, 266–274.

Ungur, G., Hrůza, J., 2017. Modified polyurethane nanofibers as antibacterial filters for air and water purification. RSC Advances 7 (78), 49177–49187.

Choi, D.Y., Heo, K.J., Kang, J., An, E.J., Jung, S.H., Lee, B.U., Lee, H.M., Jung, J.H., 2018. Washable antimicrobial polyester/aluminum air filter with a high capture efficiency and low pressure drop. Journal of Hazardous Materials 351, 29–37.

Lee, J.H., Wu, C.Y., Lee, C.N., Anwar, D., Wysocki, K.M., Lundgren, D.A., Farrah, S., Wander, J., Heimbuch, B.K., 2009. Assessment of iodine-treated filter media for removal and inactivation of MS2 bacteriophage aerosols. Journal of Applied Microbiology 107 (6), 1912–1923.

Rengasamy, S., Fisher, E., Shaffer, R.E., 2010. Evaluation of the survivability of MS2 viral aerosols deposited on filtering face piece respirator samples incorporating antimicrobial technologies. American Journal of Infection Control 38 (1), 9–17.

Woo, M.H., Lee, J.H., Rho, S.G., Ulmer, K., Welch, J.C., Wu, C.Y., Song, L., Baney, R.H., 2011. Evaluation of the performance of dialdehyde cellulose filters against airborne and waterborne bacteria and viruses. Industrial & Engineering Chemistry Research 50 (20), 11636–11643.

Joe, Y.H., Woo, K., Hwang, J., 2014. Fabrication of an anti-viral air filter with SiO 2–Ag nanoparticles and performance evaluation in a continuous airflow condition. Journal of Hazardous Materials 280, 356–363.

Park, D.H., Joe, Y.H., Hwang, J., 2019. Dry aerosol coating of anti-viral particles on commercial air filters using a high-volume flow atomizer. Aerosol and Air Quality Research 19, 1636–1644.

Park, K.T., Hwang, J., 2014. Filtration and inactivation of aerosolized bacteriophage MS2 by a CNT air filter fabricated using electro-aerodynamic deposition. Carbon 75, 401–410.

Joe, Y.H., Park, D.H., Hwang, J., 2016. Evaluation of Ag nanoparticle coated air filter against aerosolized virus: Anti-viral efficiency with dust loading. Journal of Hazardous Materials 301, 547–553.

Tellier, R., 2006. Review of aerosol transmission of influenza A virus. Emerging Infectious Diseases. 12 (11), 1657–1662.

Zumla, A., Hui, D.S., 2014. Infection control and MERS-CoV in health-care workers. The Lancet 383 (9932), 1869–1871.

Jones, R.M., Brosseau, L.M., 2015. Aerosol transmission of infectious disease. Journal of Occupational and Environmental Medicine 57 (5), 501–508.

Centers for Disease Control and Prevention, 2008. Guideline for isolation precautions: preventing transmission of infectious agents in healthcare settings. Available from: http://www.cdc.gov/ncidod/dhqp/gl_isolation.html. (Accessed 20 October 2008). .

Occupational Safety and Health Administration, 2007. Pandemic influenza preparedness and response guidance for healthcare workers and healthcare employers. US Department of Labor Publication OSHA 3328–05 Available from: http://www.osha.gov/Publications/3328-05-2007-E nglish.html. (Accessed 2 November 2010).

Yoon, K.Y., Byeon, J.H., Park, J.H., Hwang, J., 2007. Susceptibility constants of *Escherichia coli* and *Bacillus subtilis* to silver and copper nanoparticles. Science of the Total Environment 373 (2), 572–575.
Sigmon, C., Shin, G.A., Mieog, J., Linden, K.G., 2015. Establishing surrogate–virus relationships for ozone disinfection of wastewater. Environmental Engineering Science 32 (6), 451–460.
Liana, A.E., Marquis, C.P., Gunawan, C., Gooding, J.J., Amal, R., 2017. T4 bacteriophage conjugated magnetic particles for *E. coli* capturing: Influence of bacteriophage loading, temperature and tryptone. Colloids and Surfaces B: Biointerfaces 151, 47–57.
Lin, K., Marr, L.C., 2017. Aerosolization of Ebola virus surrogates in wastewater systems. Environmental Science & Technology 51 (5), 2669–2675.
Eninger, R.M., Adhikari, A., Reponen, T., Grinshpun, S.A., 2008. Differentiating between physical and viable penetrations when challenging respirator filters with bioaerosols. Clean–Soil, Air, Water 36 (7), 615–621.
Brady-Estévez, A.S., Schnoor, M.H., Kang, S., Elimelech, M., 2010. SWNT− MWNT hybrid filter attains high viral removal and bacterial inactivation. Langmuir 26 (24), 19153–19158.
Lim, J., Byun, J., Guk, K., Hwang, S.G., Bae, P.K., Jung, J., Kang, T., Lim, E.K., 2019. Highly Sensitive in Vitro Diagnostic System of Pandemic Influenza A (H1N1) Virus Infection with Specific MicroRNA as a Biomarker. ACS Omega. 4 (11), 14560–14568.
Kettleson, E.M., Ramaswami, B., Hogan Jr, C.J., Lee, M.H., Statyukha, G.A., Biswas, P., Angenent, L.T., 2009. Airborne virus capture and inactivation by an electrostatic particle collector. Environmental Science & Technology. 43 (15), 5940–5946.
USEPA Manual of Methods for Virology, 2001. USEPA Manual of Methods for Virology, Chapter 16 (EPA 600/4-84/013 N16). United States Environmental Protection Agency, U.S. Government Printing Office, Washington, DC.
Bao, L., Seki, K., Niinuma, H., Otani, Y., Balgis, R., Ogi, T., Gradon, L., Okuyama, K., 2016. Verification of slip flow in nanofiber filter media through pressure drop measurement at low-pressure conditions. Separation and Purification Technology 159, 100–107.